DOI:10.19615/j.cnki.1000-3118.2016.01.001

第54卷 第1期 古 脊 椎 动 物 学 报 pp. 1−20
2016年1月 VERTEBRATA PALASIATICA figs. 1−6

Morphology and taxonomy of *Gazella* (Bovidae, Artiodactyla) from the Late Miocene Bahe Formation, Lantian, Shaanxi Province, China

ZHANG Zhao-Qun[1] YANG Rui[1,2]

(1 *Key Laboratory of Vertebrate Evolution and Human Origins of Chinese Academy of Sciences, Institute of Vertebrate Paleontology and Paleoanthropology, Chinese Academy of Scicences* Beijing 100044 zhangzhaoqun@ivpp.ac.cn)
(2 *University of Chinese Academy of Sciences* Beijing 100049)

Abstract Fossil gazelles have been widely distributed in Eurasia and Africa during the late Neogene. They are key elements of "*Hipparion*" faunas with prominent biochronologic and ecological significance. However, no pre-Baodean age gazelle previously reported from China. We describe here in detail materials found from the Bahe Formation, Shaanxi Province, which include by far the most complete skulls and postcranials. The first fossil gazelle skeleton is mounted based on the new findings. Morphology and measurements show the similarity with *Gazella lydekkeri* from Dhok Pathan Formation of middle Siwaliks, different from the most common species *G. gaudryi*, *G. paotehensis*, and *G. dorcadoides* from Baodean age and other gazelles from Europe. Ecomorphology and measurements of long bones indicate the Lantian species, *Gazella* cf. *G. lydekkeri*, is possibly a fast runner, adapted to an open environment in Bahean age. The open environment was also suggested by faunal composition, sedimentological analysis and isotope data.

Key words Lantian, Shaanxi; Late Miocene; Bahe Formation; gazelles

Citation Zhang Z Q, Yang R, 2016. Morphology and taxonomy of *Gazella* (Bovidae, Artiodactyla) from the Late Miocene Bahe Formation, Lantian, Shaanxi Province, China. Vertebrata PalAsiatica, 54(1): 1−20

1 Introduction

The genus *Gazella* (Bovidae, Artiodactyla) is one of the most common taxa in the "*Hipparion*" faunas, widely distributed in Eurasia and Africa. The earliest gazelle fossils recovered are *Gazella* sp. from Fort Ternan of Middle Miocene (14 Ma) and *Gazella pregaudryi* from Bou Hanifia (10 Ma), Algeria (Arambourg, 1959; Gentry, 1970, 2010). Gentry (2010) also mentioned the occurrence of Middle Miocene *Gazella* from Siwaliks. The study of Chinese gazelles has a long history pioneered by Schlosser (1903) on specimens from drugstores without detailed provenances, followed by Bohlin (1935, 1939) on the

国家自然科学基金(批准号：40272009, 41072004, 41472003)、国家重点基础研究发展计划项目(编号：2012CB821904)和芬兰科学院资助。

收稿日期：2015-02-02

Lagrelius Collection kept in Uppsala, Sweden, and by Teilhard de Chardin and Young (1931) and Teilhard de Chardin and Trassaert (1938) on specimens from the Yushe Basin. Chen (1997) made a systematic revision on fossil gazelles from the Yushe Basin based on the Sino-American project collection and Licent's collection in Tianjin Natural History Museum. However, all the *Gazella* species from China previously described are recorded from the Baodean and younger ages (Chen and Zhang, 2009), leaving a long time gap for the evolution of gazelles in East Asia.

The ecological significance of gazelles was first noticed by Schlosser (1903), and greatly improved by Kurtén (1952) who emphasized the ecological significance of two species, e.g. *G. gaudryi* and *G. dorcadoides* for representatives of east wet forest and west dry steppe faunas in North China respectively. The paleodiets and habitats of these species were reinforced by stable carbon isotope evidences (Passey et al., 2007).

During 1997-2001, the Sino-Fennic joint project produced a large amount of fossil bovids, especially gazelles from the Bahe Formation, Lantian, Shaanxi Province (Zhang et al, 2002, 2013; Zhang and Liu, 2005). Of the totally 52 localities, Loc.31 yielded well preserved *Gazella* specimens, including 5 skulls and almost all postcranial elements which provide an unprecedented complete understanding of skeleton morphology and taxonomy of this taxa. This paper will describe in detail these specimens and discuss the taxonomy with brief discussion on the ecological environments.

Terminology of skull and teeth refers Chen (1997), Gentry (1966, 1970), Gray (1977). Measurement method follows Pilgrim (1937), Yang et al. (2005) and Xia et al. (2005). Comparison materials are from Natural History Museum, London, Evolution Museum of Uppsala University, Paleontological Museum of Athens University, and IVPP (Institute of Vertebrate Paleontology and Paleoanthropology, CAS).

2 Systematic paleontology

Artiodactyla Owen, 1848

Bovidae Gray, 1821

Antilopinae Baird, 1857

***Gazella* de Blainville, 1816**

***Gazella* cf. *G. lydekkeri* Pilgrim, 1937**

(Figs. 1-6)

Specimens Five almost complete skulls with lower jaws (IVPP V 15246-V 15250); together with skull V 15246 attached four cervicals (C1-C4, V 15246.1-4), and other postcranials tentatively associated for a complete skeleton (V 15246.5-76); 8 vertebrae (C5-T2, T3-T7, V 15251.1-8); 5 lumbar bones, 1 sacrum and 1 caudal (V 15252.1-7); 9 vertebrae (2 axes, 1 C5/C6, 6 lumbars, V 15253.1-9); 3 broken scapulae (V 15254.1-3); 4 pelves (V 15255.1-4); 1 partial sternum (V 15256); 7 humeri (3 complete, 2 proximal and 2 distal parts,

V 15257.1-7); 2 broken ulnae (V 15258.1-2); 1 complete and 4 partial radii (V 15259.1-5); 3 proximal and 1 distal fragments of femur (V 15260.1-4); 2 proximal and 2 distal parts of tibia (V 15261.1-4); 1 complete juvenile metacarpal, 4 proximal and 3 distal partial metacarpals (V 15262.1-8); 3 complete adult and 1 juvenile metatarsals, 2 proximal parts (one articulated with naviculo-cuboid and cuneiform) (V 15263.1-6); 4 complete articulated tarsals (V 15264.1-4); 8 carpal bones (one with the scaphoid, lunar, cuneiform, and pisiform articulated, 1 scaphoid, 2 magnums, and 1 unciform) (V 15265.1-5); 4 1st phalanges, 3 2rd phalanges (V 15425.1-7).

Locality and stratigraphic horizon Loc.31 (N34°11′04″; E109°15′04″), named as Snake Locality, found by our colleagues, Dr. Liu Liping and Prof. Mikael Fortelius, after encountering a poisonous snake and fell upon the fossils. Stratigraphically this locality locates in the middle part of the Bahe Formation. Magnetostratigraphic data indicate its age of 8.9 Ma, Bahean age (Zhang et al., 2013).

Measurements See Tables 1-3.

Description There found totally five skulls from the locality, all well preserved with lower jaws. The skull IVPP V 15246 was the least distorted, only slightly compressed on the right side, with the right parietal, right zygomatic arch, and right lower jaw lost. V 15247 was more distorted laterally, with the upper part of horn-cores and the left zygomatic arch lost, the lower jaws are well preserved. V 15248 was also compressed without the right zygomatic arch, and pterygoid preserved, lower jaws are in good conditions. The anterior part of V 15249 was compressed laterally, with the pterygoid lost, lower jaws are well preserved. V 15250 was strongly distorted, with the zygomatic arch, pterygoid lost, and the lower jaws are well preserved. V 15246 and V 15247 have horn-cores, should be males. V 15248, 15249, and 15250 have no horn-cores, are female individuals. All five skulls are adult, and V 15248 is the oldest by tooth wear.

V 15246 has almost complete horn-cores. The horn-cores are long and slender, long oval shape in cross section, with the maximum thickness leveled posteriorly to the midpoint. No keel developed. The horn-cores inserted on frontals above orbits at an angle more than 60°. The divergence is moderate at the base (on V 15247, the long axes of horn-cores form an angle about 40° measured from the base), and getting less angled upwards. The curvature is moderate. The horn-cores taper gradually towards the tip. The inner side is relatively convex than the outside. No torsion is observable. There exist moderate deep postcornual fossae.

All five skulls are similar in size without sexual differentiations (Tables 1-2), and also similar to each other in morphology but the presence of horns on males.

The skulls are medium sized, long and slender in general view. The facial part is narrow and long though with taphonomic distortion. The maximum width of skull locates at the posterior ridge of orbits. The cranial part behind the orbit is long and narrow as well, shaping the skull longer and slender. The braincase is bent downwards, with cranial axis about 30° angled to the facial axis.

Dorsal view The nasals are narrow and doomed with paralleled sides at the anterior

Table 1 Skull measurements of *Gazella* cf. *G. lydekkeri* from Lantian (mm)

	V 15246	V 15247	V 15248	V 15249	V 15250
Anteroposterior diameter/transverse diameter at base	26.5/20	32/21.5e			
Distance from anterior orbital rim to akrokranion	100		<105	96.7	
Distance from infra-orbital foramen to anterior orbital rim	43	39	39.5	<44	
Minimum length of frontal	55e		59e	55.5	
Maximum width across orbits			68	70e	
Orbital length	<37			36	
Orbital height	32.5			32.4	
Post orbital width	49e			49.6	
Braincase length: fronto-parietal suture to akrokranion	56		<58	52.3	55e
Braincase width across mastoid	48e			51	51.5
Maximum width across the occipital condyles	39		35	38	38.5
Length of tympanic bulla	24.5	25	23.9	26.8	23.6
Width of tympanic bulla	13.7	14.3	12.6	15.7	13.5
Maximum width of basioccipital across posterior tuberosities	21.7	20.6	20.5	20	
P2-M3	54	55.5	53.7	52.8	54.2
P2-P4	21.7		23	22.2	22.5
M1-M3	33.4	32.6	33.8	32.2	33
Maximum length of mandible				148	
Length of diastema				37	
Mental foramen to p2	25.5		24	24.7	22.5
Height of vertical ramus	68.5	>68			
p2-p4	19.7	21.2	20.8	19	22.2
m1-m3	35.7	37.4	36.2	34.9	37.2
p2-m3	55.4	58.2	56.2	54	58.3

Note: e. estimated value.

Table 2 Tooth measurements of *Gazella* cf. *G. lydekkeri* from Lantian (mm)

	V 15246	V 15247	V 15248	V 15249	V 15250	*G. lydekkeri*
p2	5.2	6.0	6.6	4.7	6.1	6
p3	7.4	7.1	6.0	7.0	7.4	8.5
p4	8.4	8.4	8.9	8.2	8.5	9.5
m1	9.2	9.7	8.9	9.4	8.8	10
m2	10.8	11.7	10.8	10.3	11.7	13
m3	16.6	15.4	16.6	15	16.0	17.5
P2	7.2	7.9	7.0	6.7	7.4	10
P3	6.6	8.2	6.9	6.8	7.0	8
P4	7.2	7.1	7.2	7.2	6.9	7
M1	10	10	8.8	9.4	8.7	11
M2	12.6	12.2	10.5	12.2	13	13.5
M3	12.1	11.7	13.2	12.0	13.3	15

Note: measurements of *Gazella lydekkeri* (AMNH 19663) cited from Pilgrim (1937).

part, widened at the middle way, then tapered in between the developed nasal processes of frontals (Fig. 1A). The posterior end of nasal extends to the level of the frontal edge of orbit. The anterior part of frontal depressed slightly and the posterior part elevated along the suture. The supraorbital foramina locate at the base of horn-core on males, above the orbital roof on females with anteroposteriorly extended surrounding pits. Dorsal orbit rim is wide (Fig. 2A). The parietal-frontal suture is straight and wide. The parietal gets to narrower posteriorly

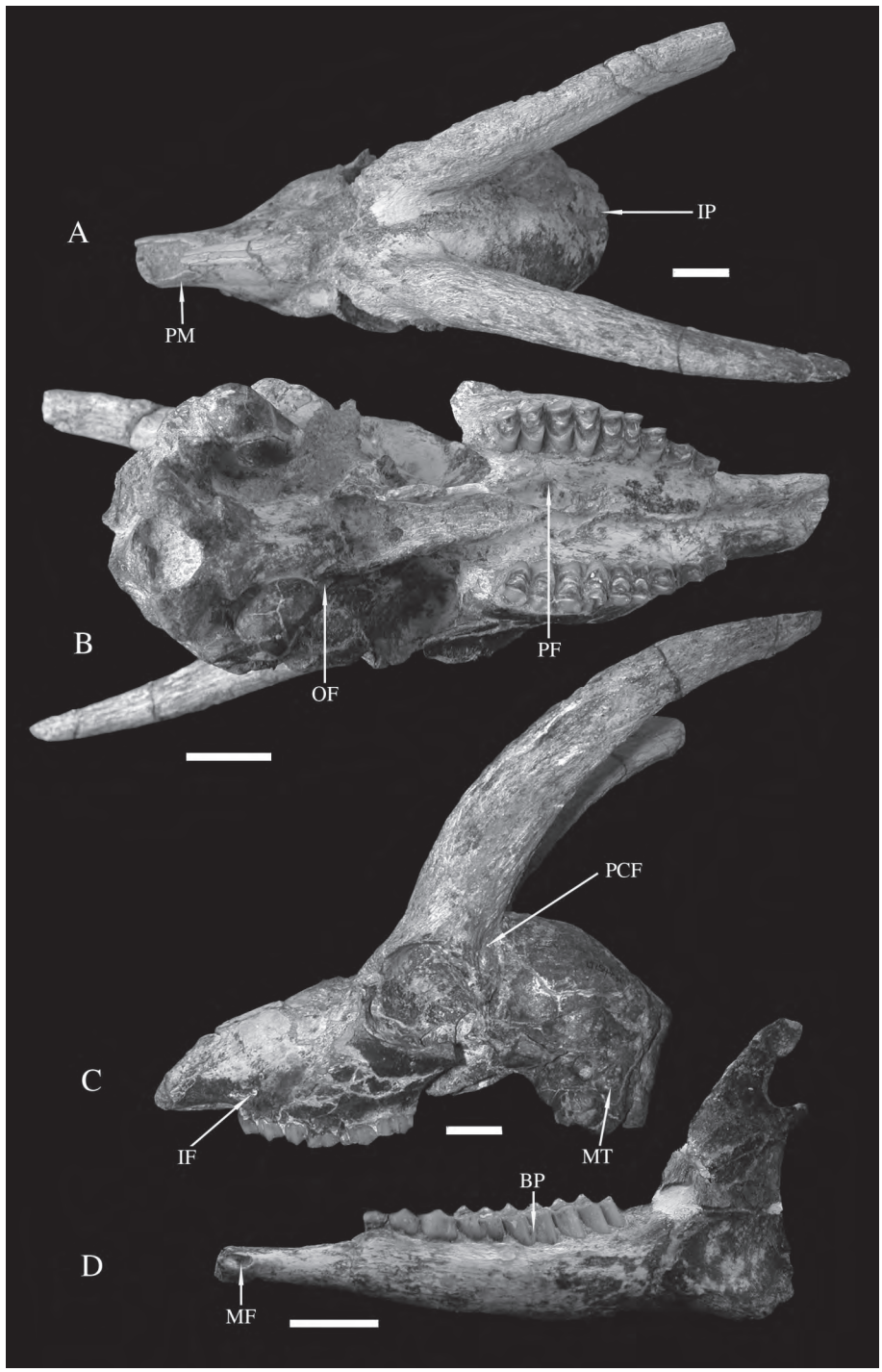

Fig. 1 Skull and mandible of *Gazella* cf. *G. lydekkeri* (IVPP V 15246) from Lantian
A-C. skull: A. dorsal view, B. ventral view, C. left side view; D. labial view of the left mandible. Scale bars=2 cm
Abbreviations: BP. basal pillar; IF. infraorbital foramen; IP. interparietal; MF. mental foramen; MT. mastoid; OF. oval foramen; PCF. postcornual fossa; PF. palatine foramen; PM. premaxilla

with observable temporal ridges on both sides leading to the minimum distance at the parietal-interparietal suture. The interparietal is narrow anteriorly and contacts with mastoid posterolaterally by the posterior extension. The occipital face has a prominent median crest, which makes each side of occipital surface facing lateroposteriorly.

Lateral view The premaxilla is thin and narrow plate like, strongly inclined and contacts the nasal at the vertical level slightly anterior to P2 (Fig. 1A). The maxillae get to narrower anteriorly in front of tooth rows and widen posteriorly to the maximum width at the level of maxillary tuberosities. The preorbital fossa is moderately deep with developed lachrymal bone. There exists an ethmoidal fissure between the lachrymal and the nasal. The infraorbital foramen opens anteriorly, situates above P2 at a low position (Fig. 1C). The maxillary tuberosity, above M1, is moderate in size. The orbit fossa is round shaped, with well developed upper and lower ridges. The upper orbit ridge is lower than the highest point of the skull, which is positioned at the posterior part of the frontals. The anterior ridge of orbit levels with the M3 paracone. The zygomatic arch posterior to the orbit is short. The zygomatic process of squamosal is long and wide with a saddle like morphology for articulation with the coronoid process dorsally and condylar process ventrally. There exists a large postglenoid foramen. The tympanic bulla is large, round in lateral view with short acoustic meatus. The oval foramen is large, round and open laterally at the posterior end of lateral plate of pterygoid (Fig. 1B). The jugular process extends downwards, tightly encloses the posterior surface of tympanic bulla (Fig. 2C), and anterodorsally contacts the mastoid, which is visible in lateral view.

Ventral view No incisive foramen preserved on all five skulls. The palatal ridges in front of tooth rows approach but do not touch. The palatine foramen locates at the level of posterior lobe of M2 (Fig. 1B). The maxilla width gets to maximum at the level of M2 and greatly diminishes forwards from P4. The median palatine indentation (choana) is anterior to the lateral ones and especially on female individuals (Fig. 2B). The basioccipital is long quadrate in shape with weakly developed and laterally extended posterior tuberosites on male individuals, the anterior tuberosities are even weaker, and the groove between them is extremely shallow. On the female individual, the basioccipital is slightly narrower and with slightly larger anterior tuberosites. The tympanic bulla length does not exceed that of the basioccipital.

The mandible ramus is also long and slender (Fig. 2D). The inner side is flat, and the outer side is outbowed, and thickness of the horizontal ramus increases posteriorly. The symphysis is short, extends to the level of the mental foramen. The mental foramen is long oval shaped, posterior to the canine. The diastema is longer than the molar row. The coronoid process is high and curved posteriorly, with a slightly concave inner side and flat outer side. The condyle is below the highest point of coronoid process, separated by a deep notch (Fig. 2D). The angular process extends slight away to the posterior edge of the vertical ramus.

The premolar row is relatively short (Fig. 3; Table 1). P2 is very small in size; the paracone is large with a rib. P3 is very similar to P2, but shorter. P4 has a triangle shaped

Fig. 2 Skull and mandible of *Gazella* cf. *G. lydekkeri* (IVPP V 15249) from Lantian
A–C. skull: A. dorsal view, B. ventral view, C. left side view; D. labial view of the right mandible. Scale bars=2 cm
Abbreviations: AM. acoustic meatus; CN. choana; CP. condyle process; CRP. coronoid process;
JP. jugular process; PCF. postcornual fossa; PTB. posterior tuberosity of basioccipital;
SOF. supraorbital foramen; TB. tympanic bulla; TR. temporal ridge; ZM. zygomatic plate

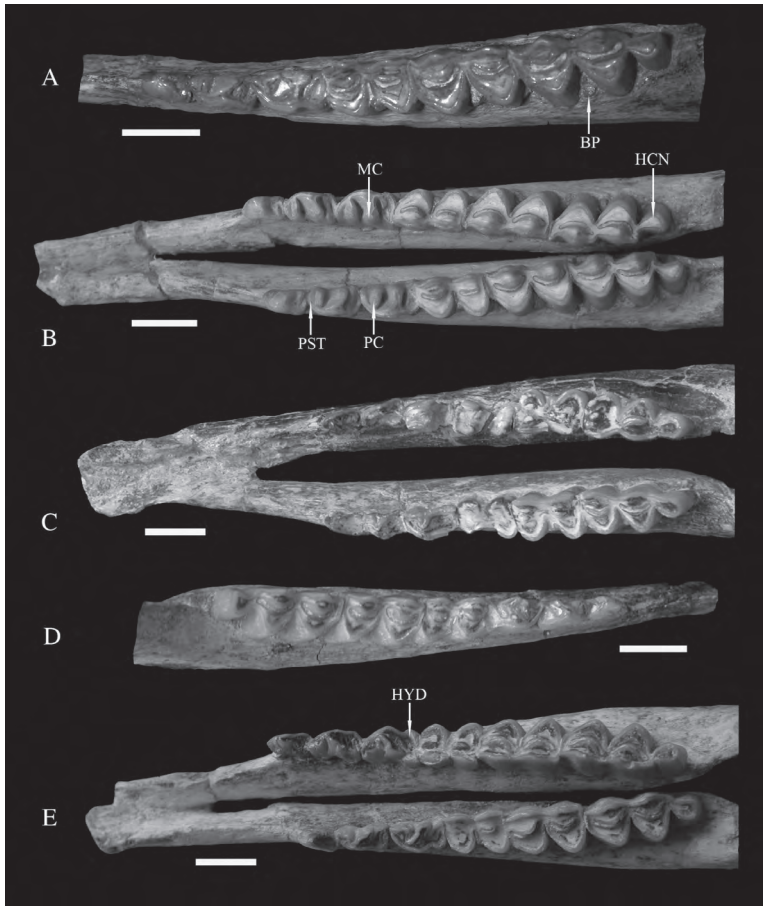

Fig. 3 Occlusal view of mandibles of *Gazella* cf. *G. lydekkeri* from Lantian
A. IVPP V 15246, B. V 15247, C. V 15248, D. V 15249, E. V 15250. Scale bars=1 cm
Abbreviations: BP. basal pillar; HCN. hypoconulid; HYD. hypoconid; MC. metaconid; PC. paraconid; PST. parastyle

occlusal surface. The paracone is large. There is parastyle, however, the metastyle is weak. The protocone is located in the middle line, with the anterior and posterior ridges to form the triangle shape together with the labial cusps. The molars are basically quadrate in shape. The size increases from M1 to M3. On M1-2, there are small lingual basal pillars. Labial styles are developed, of them the mesostyle is the largest. The rib between the parastyle and mesostyle is more developed than the posterior rib.

The i1 is shovel shaped, with a straight medial side, and flanged distal side. The i2 is long rectangular in shape, and much smaller than i1. There preserved only the root of i3 on V 15249. The canine exists by preservation of its root, and extends anteriorly by the direction of root, possible having the shape of incisors. The p2 is small with a simple occlusal structure. The protoconid is the main cusp, and the paraconid is much lower and not well separated from the protoconid. The p3 is significantly larger than p2. Its paraconid is well separated

from protoconid, and not connected with parastyle and metaconid. The metaconid extends posterolingually, but does not contact with entoconid. The protoconid is slightly more anterior than the metaconid, and the hypoconid is not enlarged. The p4 has rather derived looking characters, e.g. the metaconid extends anteriorly and connects with the paraconid in later wear, and posteriorly connected with the entoconid. The hypoconid is prominent, with a furrow separating with the protoconid on labial side. There exists hypoconulid, which connects with the entoconid. The paraconid extends posterolingually and well separated from the parastyle. Lower molars have basal pillars on buccal sides, which are more developed on males than on female individuals. The basal pillar decreases from m1 to m3. The goat folds are almost indistinguishable. The m3 has a large and labially offset third lobe, and developed anterior cingulum.

With skull V 15246, four cervical bones attached in situ. The other four skulls attached with atlases respectively. The atlas is trapezoid in outline with narrower proximal and wider distal side (Fig. 4A). The articulate fossae with the occipital condyles are deep and laterally bounded, separated by a shallow and wide notch dorsally, and wider and deeper U shaped notch ventrally. There developed two separate depressions by a central ridge at the anterior one third of dorsal arch. The ventral arch presents a median tubercle. The transverse processes are thin plate like, extending posterolaterally to form a sharp spike. The alar foramen is round without groove in dorsal view.

The axis (Fig. 4B) is longer than wide, with high and plate like spinous process dorsally, while the body is not developed, about half length of the axis. The odontoid process is C shaped surrounded by well developed saddle like articular facet. The transverse process flanges posterolaterally. The ventral ridge extends cranially but does not reach the level of the collar. The vertebral artery foramen opens obliquely, posteroventrally to it a smaller foramen opens anteriorly.

The third cervical (C3) is slightly shorter but stronger than the axis. The transverse processes are think plate shape, with longer length than the body, and lateral flange posterolaterally protruding. The ventral ridge in the middle of the surface is complete across the body. The dorsal arch is rectangular shape with four equally sized articular processes. The fourth cervical (C4) is similar to the third in morphology and size except the dorsal arch wider with stronger articular surfaces, and the transverse processes not confluent anteroposteriorly.

C6 has a more slender spinous process, and anteriorly pointed, more constrained lateral side of dorsal arch, and rod like transverse process which is more anteriorly positioned.

Different from the previous cervical bones, C7 has well developed spinous process which has same basal length with the dorsal arch and getting triangle shape from the mid height. The caudal width across the posterior articular processes is narrower and shorter than on the previous cervical.

The first thoracic (T1) is characterized by a saber shaped dorsal spine, and the presence

of anterior articular processes which are smaller than on the cervicals. Inferior to the transverse process there developed a saddle like articular facet for the tubercle of rib. The transverse processes and facets are getting smaller in the posterior thoracic bone. The last thoracic (T13) is more like a lumbar except having anterior costal pits and triangle shaped transverse processes.

Lumbars are similar in structure, tightly articulated each other with hook like articular processes, having flat wing like transverse processes. From the first to the last lumbar (L7), the body and dorsal arch get to shorter and wider from rectangular towards more square shape. The posterior articular surface of the body becomes wide oval shape to fit the anterior articular surface of the sacrum body.

The sacrum consists of four sacral elements (Fig. 4D). It has larger and more anteroposteriorly elongated hook like articular surfaces with the lumbars. The wing is roughly round shape, facing posterolaterally. The width of sacrum gets to narrow sharply posterior to the wing and minimum at the third sacral bone. The medial ridge is well united and forms a wall like plate with slightly enlarged dorsal roof.

Ribs are not well preserved because of the slenderness. The first rib is slightly curved. It has large tubercle articulated tightly with the saddle like facet of the first thoracic. The head is almost horizontally orientated with a long neck. The rib body gets to flatter and wider downwards.

There also preserved a partial sternum, which is flat plate like with a long rod shape xiphoid process (Fig. 4F).

The scapula (Fig. 4C) is triangle in shape. The spine is prominent, located anteriorly, with the central part curved. The glenoid fossa is round without obvious notch. The articular surface is at the same level with acromion.

In lateral view the humerus shaft is moderately curved, with the proximal posteriorly and distal anteriorly (Fig. 5A). The deltoid tuberosity is low and ridge like. The humerus head is large and round in shape. The greater tubercle is prominent and much higher than the lesser tubercle, and the intertubercular sulcus in between them is wide and shallow. The distal end of humerus extends laterally, with developed trochlea. The lateral epicondyle is larger than the medial epicondyle. The olecranon fossa is deep bounded by developed epicondylar ridges.

The ulna is almost fused with the radius in proximal end and leaves space downwards in the middle of the shaft. The proximal part above the trochlear notch is a thin and rectangular plate in lateral view with slightly curved posterior edge.

The radius is also moderately curved in lateral view as the ulna. The posterior surface of the shaft gets to flat or slightly concave in the middle part. The proximal head is short and wide, extending laterally with the medial part slightly longer than the lateral end. At the distal part, there exist two dorsal low ridges which are parallel each other.

The carpal bones are tightly in situ and not separated (Fig. 4I). The scaphoid is rectangular in medial view, anteroposteriorly longer than high, articulated proximally with the

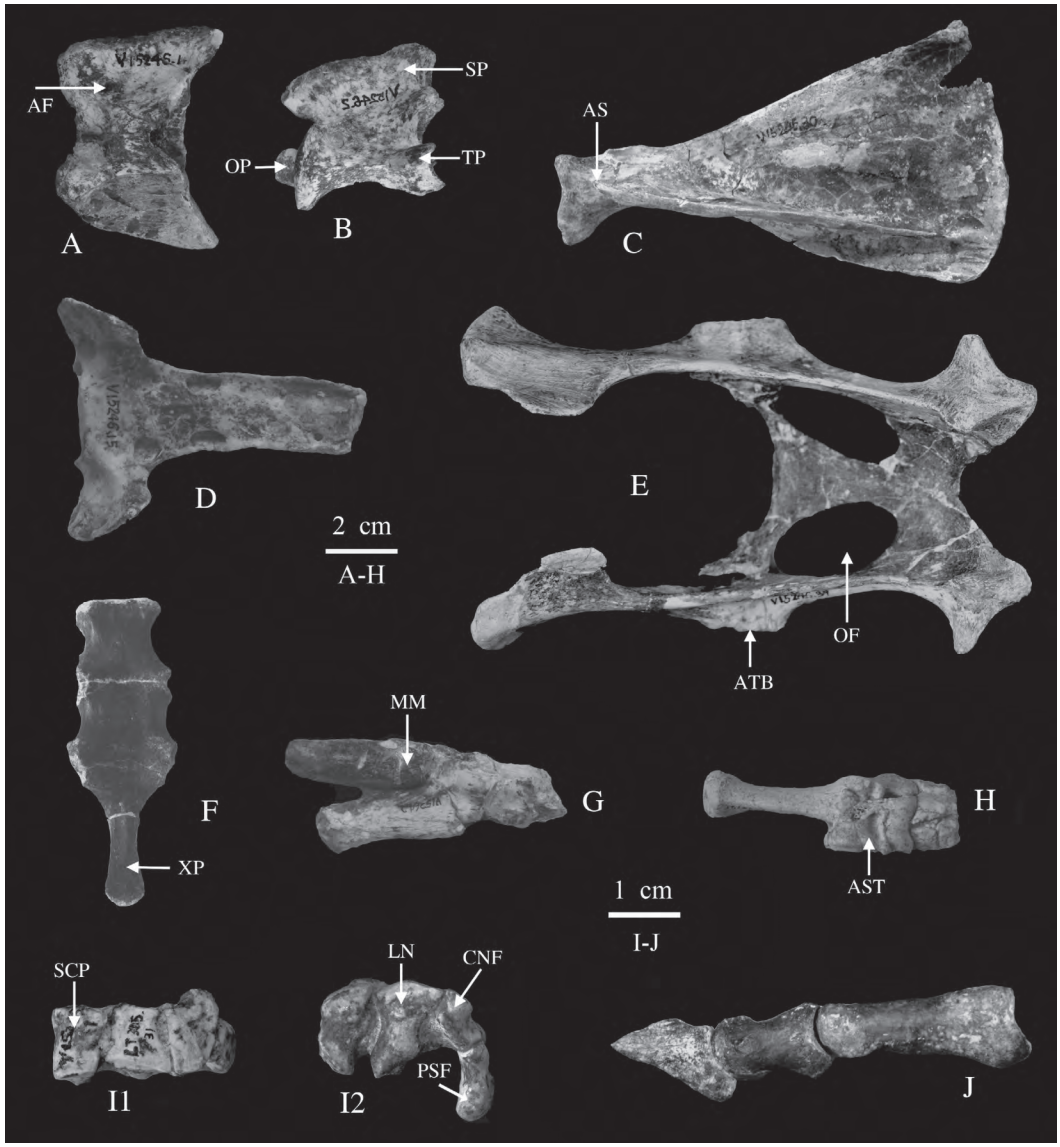

Fig. 4 Postcranials of *Gazella* cf. *G. lydekkeri* from Lantian

A. dorsal view of atlas (IVPP V 15246.1); B. lateral view of axis (reverse, V 15246.2); C. dorsal view of right scapula (V 15246.30); D. ventral view of the sacrum (V 15246.15); E. dorsal view of pelvic (V 15246.39); F. ventral view of sterum (V 15256); G. lateral view of tarsal with distal part of tibia (V 15264.2); H. dorsal view of the tarsal (V 15264.1); I. carpal (V 15265.1): I1. anterior view, I2. distal view; J. lateral view of left phalanges (V 15246.76)

Abbreviations: AF. alar foramen; AS. acromion of scapula; AST. astragalus; ATB. acetabulum; CNF. cuneiform; LN. lunar; MM. median malleolus; OF. obturator foramen; OP. odontoid process; PSF. pisiform; SCP. scaphoid; SP. spinous process; TP. transverse process; XP. xiphoid process

medial end of radius. The lunar locates in between the scaphoid and cuneiform, and articulates with the lateral end of radius, and both the magnum and unciform distally.

The metacarpal is about the length of the radius (Table 3), and the shaft is slightly curved

in lateral view. There exists a developed and wide groove on the plantar surface. On the dorsal surface at the distal part there is a slight vascular groove. The proximal articular surface is triangle shape, with developed metacarpal tuberosity. Two articular surfaces with sagittal ridge are separated by a deep intertrochlear notch.

Table 3 Length of long bones of *Gazella* cf. *G. lydekkeri* from Lantian (mm)

	femur	tibia	metatarsal	humerus	radius	metacarpal
V 15246	164	204		124	142	141
V 15257.1				122		
V 15257.2				122		
V 15259.1					155	
V 15263.1			167			
V 15263.2			168			
V 15263.3			169.5			

The pelvic is almost complete with only slightly loss at the iliar wing (Fig. 4E). The articular surface with the sacrum is flat. The ventral side of the ilium body is straight and end with a deep fossa anterior to the acetabulum, which located in the middle of the ilium and ischium. The greater sciatic notch is obtuse incised. The lesser sciatic notch is very shallow. There developed three tubercles at the posterior end of ischium, of them the lateral one is the largest. The obturator foramen is long oval shaped. The pubis is L shaped with a ridge developed along the pelvic symphysis.

The femur (Fig. 5B) head is round and bulky in the medial part and the articular surface gets to narrower and constrained laterally toward the level of middle line of the femur shaft. The greater trochanter is rectangular plate like in lateroposterior view, and the proximal end higher than the femur head. The notch in between them is narrow. The lesser trochanter is moderately developed and connected with the greater trochanter by a crest, which enclose the deep trochanteric fossa. The femur shaft is slightly curved in lateral view. The medial trochlear ridge is thicker and higher than the lateral ridge and extends more proximately. The trochlear ridges extend obliquely with the long axis of the shaft, with an angle about 20°. The lateral condyle is more robust than the medial one, and both are obliquely elongated, however, with reversed direction with the trochlear ridges.

The tibia is the longest limb bone (Fig. 5C). The proximal part is stronger with developed tibial tuberosity and high crest extending downward to the one third of the shaft. The medial side of the crest is flat and lateral side concave. The cross section of the shaft near the proximal part is triangle in shape and turns to be rectangular shape distally. With the developed tuberosity, the proximal articular surface is a sharp triangle, incised laterally by the extensor groove. The intercondylar tubercles are prominent. The lateral articular surface with femur condyle is slightly larger than the medial one by extension of the posterolabial corner of the triangle. Below this protrusion, there fused the proximal part of vestige fibula. At the distal end, two deep sagittal orientated trochlear grooves separated by a central ridge. The medial groove is narrow and longer than the lateral one and bounded medially by the medial malleolus, which

Fig. 5 Long bones of *Gazella* cf. *G. lydekkeri* from Lantian
A. right humerus (IVPP V 15246.32); B. right femur (V 15246.40); C. right tibia (V 15246.42); D. right radius (V 15246.22); E. right metacarpal (V 15246.38); F. right metatarsal (V 15263.1)
A1-F1. anterior view; A2-F2. posterior view. Scale bar=2 cm

is spike like and protrudes downwards and articulates with the medial surface of astragalus.

The calcaneum is robust built with medial-laterally compressed body. The calcaneal tuberosity is prominent dorsally and triangle shape, while ventrally there developed a trochlear shape groove. The anteroposterior length of the calcaneum body gets to longer and reaches the maximum below the sustentaculum. The articulate surface with the medium malleolus has similar size proximal convexity and distal concavity (Fig. 4G, H).

The metatarsal is about 20% longer than the metacarpal. The cross section of the shaft is

subrectangular, with width slightly shorter than the length (Fig. 5F). There is a wide and deep groove on the dorsal surface of the shaft. The proximal articulate surface is pentagonal shape. The distal end consists of two similar sized articulate trochleae.

The phalanges of hand and foot in bovids are very similar in shape and size (Sisson, 1914). Before further analysis, we describe them together as phalanges. The first phalanx is the longest one with slightly convex lateral surface and flat medial side. The proximal articulate surface is divided into two parts by a deep central groove. The lateral part is larger than the medial part. The first and second phalanxes have similar distal morphology, centrally separated into two articulate surfaces. The second phalanx is about two thirds of the first phalanx in length. The third phalanx is triangle shape diminishing distally (Fig. 4J).

Based on the materials described, we mounted a complete skeleton using casts of the specimens (Fig. 6) with only some ribs and tails reconstructed referring living goats.

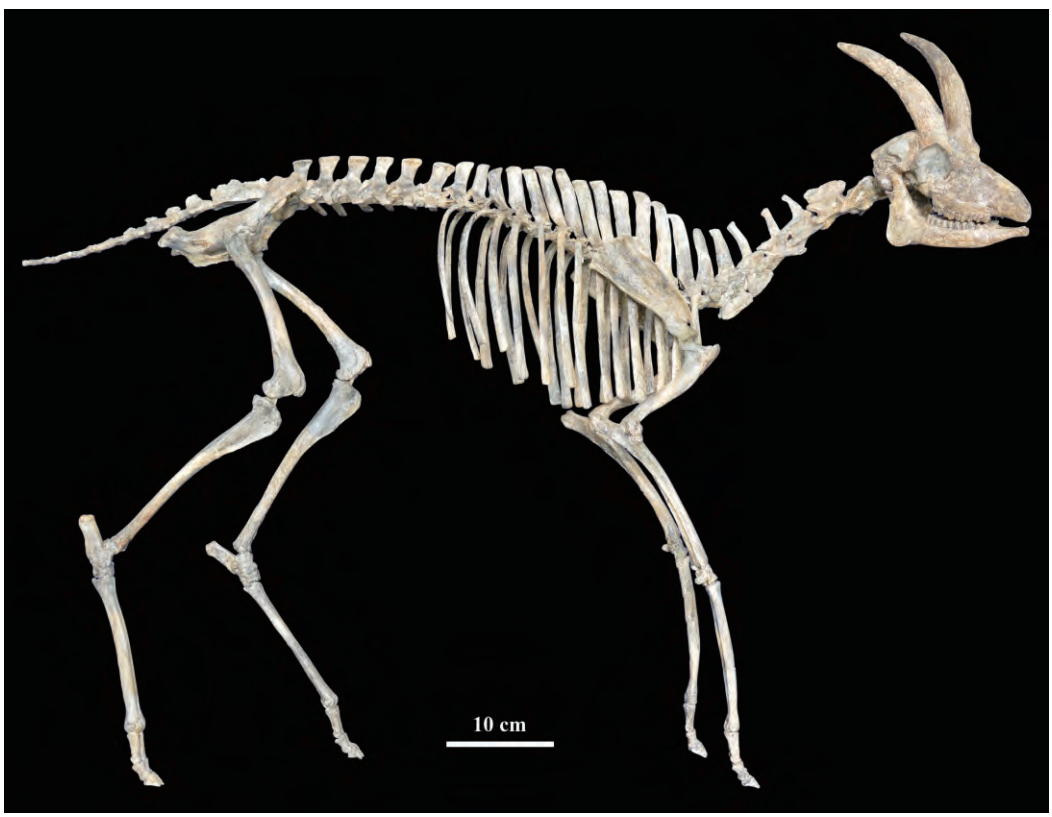

Fig. 6 Mounted skeleton (cast) of *Gazella* cf. *G. lydekkeri* from Lantian mainly based on IVPP V 15246 and reconstructions on other referred specimens
Courtesy of Mr. Cao Qiang and his colleagues for the reconstruction and mounting

3 Comparison

All the five skulls with jaws have similar size (Table 1-2) and morphology except the males having horns. One way ANOVA analysis of the tooth measurements confirms no significant differentiations. Hence, they can readily be attributed into one species.

The specimens here described have similar size with the female skull of *Dorcadoryx orientalis* (IVPP V 14423) from the same formation (Chen, 2005: fig. 1B), however their cheek teeth are proportionally smaller than the latter species. Although dorsal-ventrally distorted, V 14423 shows shallow preorbital fossae and wider snout by less forward diminishing at the premolar rows. The horn-cores from the frontlets of *Dorcadoryx orientalis* are also larger and tapering faster upwards.

The morphology of the Lantian species has characters of the most common bovid genus *Gazella* as listed by Gentry (2010), e.g. size small with moderate long horn-cores, the level of mediolateral width lying slightly behind the anteroposterior midpoint, without keels or torsion, of oval shaped cross section, the lateral surface flatter than the medial, moderately upright insertions, backward curved, placed the back of the orbits. There developed postcornual fossa, no sinuses within the frontals, braincase not shortened, occipital surface with each half facing partly laterally as well as backward, large tympanic bullae, m3 with large third lobe.

Fossil gazelles are rich in the "*Hipparion*" faunas. There have recorded more than a dozen species.

From Chinese Late Miocene, three species (*Gazella gaudryi*, *G. dorcadoides* and *G. paotehensis*) are the most common taxa, and in detail studied (Bohlin, 1935; Teilhard de Chardin and Young, 1931). Table 4 shows comparison with them based on observation of the specimens in the Lagrelius collection. Though with many similarities, the differences between the Lantian species and these three species are obvious.

The Lantian specimens are, however, more similar to *Gazella lydekkeri*, described by Pilgrim (1937), from the Dhok Pathan Formation of middle Siwaliks. They share many characters as following: females have no horn-cores; long and slender skull, with deep preorbital fossa and narrow face, the premaxilla extends back to the level of P2, the braincase longer than the width, face bent down on cranial axis at about 35°; The occipital surface is not flat, with a prominent median crest, terminating above in a knob-like swelling with flattened depressions on either side of it; tympanic bulla laterally flattened. The horn-cores have relatively flat lateral side and convex median side. The cross-section is basically oval or subtriangular. Molars have basal pillars, and p4 has hypoconulid separated with entoconid in early wear stage. The third lobe of m3 offsets labially. However, the Lantian specimens have some different characters: braincase more heavily bent down, horn-cores more compressed laterally, more divergent and less inclined, and relatively less closely set, lower mandible more slender, molars having goat folds less developed, ribs on upper and lower molars less developed, especially on P4 and last molars, the premolar row shorter relatively, and less

Table 4 Morphological comparisons with three species of *Gazella* from Chinese Late Miocene

Characters	*Gazella* cf. *G. lydekkeri*	*G. paotehensis*	*G. gaudryi*	*G. dorcadoides*
Female with horns or not	no	no	no	no
Cross section of horn-core	oval	oval	oval to round	round
Maximum transverse width	posterior	middle	middle	middle
Horn-cores compressed laterally	yes	moderate	no	no
Horn-cores inclination	moderate	moderate	moderate	strong
Horn-cores divergence	moderate	moderate	slightly	slightly
Horn-cores with longitudinal grooves	shallow	moderate	shallow	shallow
Postcornual fossa	deep	deep	deep	deep
Dorsal orbital rim	wide	wide	wide and horizontal	wide and horizontal
Frontal sinuses	no	no	no	no
Cranial roof inclined or curved posteriorly	inclined	hind part curved	curved	hind part inclined
Inter-frontal suture complicated	hind part complicated	complicated	hind part complicated	hind part complicated
Supraorbital foramina with surrounding pits	yes	yes	yes	yes
Length of braincase	long	short	long	short
Braincase sides widening	no	yes	no	yes
Temporal ridges approach	strongly posteriorly	strongly posteriorly	less	less
Lachrymal size	large	large	large	large
Maxillary tuberosity prominent	yes	yes	yes	yes
Ethmoidal fissure	yes	yes	yes	yes
Preorbital fossa	deep and wide	shallow and wide	deep and wide	deep and wide
Posterior tip of nasals surpass the level of orbital anterior rim	no	no	just reach the line	just reach the line
Infra-orbital foramen	P2	P2	P2	P2
Premaxilla contacting nasals or not	yes	yes	yes	yes?
Palatine foramina at the level of	M2	M2/M3	M2	M2
Auditory bulla	large	long and narrow	long and narrow	small and round
Basioccipital, shape	subrectagular	rectangular	rectangular	rectangular
Anterior tuberosities of basioccipital, size	large	small	large	varies
Foramina ovalia size, open	large, lateral	large	–	–
Occipital surface faces laterally or posteriorly	laterally	slightly posteriorly	slightly laterally	slightly laterally
Mastoid exposure wide or narrow	wide	wide	wide	narrow
Mastoid contacts parietal	no	no	yes on female, no on male	no
Cheek teeth hypsodonty	mesodont	mesodont	mesodont	hypsodont
Length of premolar row less than 60% molar row	less		more	less
p3 metaconid ridge, oblique or transverse	oblique	oblique	oblique	oblique
Paraconid of p3+p4 indistinct or well separated from parastylid	distinct	distinct	distinct	indistinct
p4 with labial origin of metaconid situated posterior to protoconid	yes	yes	yes	yes
p4 with shallow or deep valley anterior to hypoconid	shallow	deep	shallow	deep

Continued

Characters	*Gazella* cf. *G. lydekkeri*	*G. paotehensis*	*G. gaudryi*	*G. dorcadoides*
Metaconid-entoconid fused or not on p4	no	yes in later wear	no	yes for young
Paraconid-metaconid fused or not on p4	variable	yes in early wear	no	no
m3 with extension of lingual wall posteriorly	yes	no	no	slightly
Upper molar mesostyles strong and with concave labial wall of metacone behind	no	yes	no	yes
M3 metastyle as a flange	no	no	no	slightly
Labial ribs between the styles on upper molars	week	week	week	no
Ectostylids on lower molars (basal pillar)	m1-m3	m1	m1-m3	no, even on very worn teeth
Lower molars with outbowed or flat lingual walls	outbowed	outbowed	slightly outbowed	flat
Lower molars with or without goat folds	no	no	no	no

prominent basioccipital tuberosities and no groove between them. Considering of the unknown individual variation of *Gazella lydekkeri*, we tentatively assign the Lantian specimens as *Gazella* cf. *G. lydekkeri* herein.

The Lantian species is distinct from *Gazella capricornis* form Pikermi, Greece in having less robust and more median-laterally flattened horn-cores, and relatively larger teeth. Compared with *G. deperdita* from Cucuron, France, the Lantian species has longer horn-cores, with the anteroposterior length decreasing gradually from the base to tip, and more straight insertion above the orbit, and also differs from *G. deperdita* which has strong posteriorly narrow horn-cores. The Lantian species differs from the Samos species *G. mytilini* in the latter having hinder half of the orbit situated beneath the horn-core, horn-cores parallel each other, more hypsodont teeth, basal pillars on molars wholly lacking etc. Different from *G. pilgrimi*, the Lantian species has more curved horn-cores, premolar row relatively shorter and basal pillars more developed on molars.

4 Discussion and conclusion

Bovid fossils from Chinese Middle Miocene are relatively rare and less diversified than from the Late Miocene. Only three genera, *Eotragus* of Bovinae, *Kubanotragus* of Hippotraginae and *Turcocerus* of Urmiatheriinae were documented previously (Chen and Zhang, 2009). The gazelle fossils found from Bahe Formation are the earliest records of Antelopinae in China.

Systematic study on all species of *Gazella* is still pending and out of the scope of this paper. Nonetheless, it is hardly to relate the Lantian species with all the later occurred species from China with some seemingly derived characters, e.g. short premolar row, enlargement of metaconid on p4, compressed oval shaped cross section of horn-core, long and bent downward

braincase etc.

Kurtén (1952) analyzed the "*Hipparion*" faunas found from Chinese Late Miocene, indicating the ecological significance of the high crowned *Gazella dorcadoides* and low crowned *Gazella gaudryi*, representing west dry and east humid realm in North China respectively. By tooth crown height, the Lantian species is intermediate between these two species, showing no strong diet preferences.

However, the Lantian species with slim and elegant body plan may indicate its good running ability. The femur has long and horizontal neck of femur head, deep notch between the head and greater trochanter, wide distal articulation and anteriorly projected median ridge. The tibia has prominent tubercles on the proximal articulation surface and two sagittally orientated deep trochlear grooves separated by a central ridge at the distal end. The metatarsal and metacarpal both have same size and paralleled articulate trochleae. The proximal articulate surface of first phalanx is divided into two parts by a deep central groove. All these but least characters indicate the adaptation of running forward fast without much flexibility of turning around (Gentry, 1970). The length ratios of radius/humerus and tibia/femur are roughly 120%, also suggest their fast running ability (Osborn, 1929). The fast running lifestyle possibly suggests an open environments during their living time period, consistent with the ecological pattern of Bahean Fauna (Zhang et al., 2002; Zhang, 2006), based on sedimentological study (Kaakinen and Lunkka, 2003) and isotope data (Kaakinen et al., 2006).

The bovid assemblage from the Bahe Formation, together with *Shaanxispira baheensis*, *Dorcadoryx orientalis*, *Lantiantragus longirostralis* (Zhang, 2003; Chen, 2005; Chen and Zhang, 2004) is in sharp contrast with the much more diversified assemblage of Baodean age (Chen and Zhang, 2009). The turnover of the bovid assemblage across the Bahean/Baodean fit the climatic and ecological change scenario suggested by Kaakinen et al. (2006) and Zhang et al. (2013).

Acknowledgements The authors sincerely thank all participants in the Lantian project for the discovery and excavation of the fossils described in this paper. Professor Chen Guanfang from IVPP provides critical comments and suggestions which highly improve the draft. ZZQ appreciates help from his senior colleague and mentor, Dr. Alan Gentry, when he visited Natural History Museum, London in 2002 as a newcomer. He also indebts to Dr. Solweig Stunes, recently deceased curator of Evolution Museum of Uppsala University for hosting his visits and study on the Lagrelius collection.

陕西蓝田灞河组晚中新世*Gazella*羚羊的形态特征与分类

张兆群[1] 杨 睿[1,2]

(1 中国科学院脊椎动物演化与人类起源重点实验室，中国科学院古脊椎动物与古人类研究所 北京 100044)

(2 中国科学院大学 北京 100049)

摘要：*Gazella*羚羊是“三趾马动物群”中常见成员，在晚中新世至更新世地层中广泛分布，演化速率相对较快，具有重要的生物地层学及生态指示意义，但在我国尚未有保德期之前的化石报道。本文研究的化石发现于陕西蓝田灞河组中部，磁性地层学资料显示其年代为晚中新世灞河期。化石标本包括了5个近乎完整的头骨、下颌以及颅后骨骼。根据发现的标本装架起第一个完整的*Gazella*羚羊骨架。形态对比与测量数据表明，蓝田标本与巴基斯坦西瓦里克发现的*Gazella lydekkeri*非常相近，而不同于欧洲晚中新世常见的*Gazella*各种以及我国发现的种类。从肢骨的形态分析与测量比例数据来看，*Gazella* cf. *G. lydekkeri*适合快速奔跑运动，可能生活在相对开阔的环境中，与灞河期动物群的生态类型以及与灞河组沉积学、同位素地球化学等研究所指示的相对干旱、半干旱的开阔草原环境相一致。

关键词：陕西蓝田，晚中新世，灞河组，羚羊

中图法分类号：Q915.876 **文献标识码**：A **文章编号**：1000−3118(2016)01−0001−20

References

Arambourg C, 1959. Vertébrés continentaux du Miocène supérieur de l’Afrique du Nord. Publ Serv Carte Géol Algérie, n s, Paléont, Mém, 4: 1–159

Bohlin B, 1935. Cavicornier der *Hipparion*-Fauna Nord China. Palaeont Sin, Ser C, 9(4): 1−166

Bohlin B, 1939. *Gazella* (*Protetraceros*) *gaudryi* (Schlosser) and *Gazella dorcadoides* Schlosser. Bull Geol Inst Uppsala, 28: 79−122

Chen G F, 1997. The genus *Gazella* Blainville, 1816 (Bovidae, Artiodactyla) from the late Neogene of Yushe Basin, Shanxi Province, China. Vert PalAsiat, 35(4): 233−249

Chen G F, 2005. *Dorcadoryx* Teilhard et Trassaert, 1938 (Bovidae, Artiodactyla) from the Bahe Formation of Lantian, Shaanxi Province, China. Vert PalAsiat, 43(4): 272−282

Chen G F, Zhang Z Q, 2004. *Lantiantragus* gen. nov. (Urmiatheriinae, Bovidae, Artiodactyla) from the Bahe Formation, Lantian, China. Vert PalAsiat, 42(3): 205−215

Chen G F, Zhang Z Q, 2009. Taxonomy and evolutionary process of Neogene Bovidae from China. Vert PalAsiat, 47(4): 265−281

Gentry A W, 1966. Fossil Antilopini of East Africa. Bull Br Mus (Nat Hist) Geol, 12: 43−106

Gentry A W, 1970. The Bovidae (Mammalia) of the Fort Ternan fossil fauna. In: Leakey L S B, Savage R J G eds. Fossil Vertebrates of Africa. London and New York: Academic Press. 243−323

Gentry A W, 2010. Bovidae. In: Werdelin L, Sanders W J eds. Cenozoic Mammals of Africa. Berkeley and Los Angeles: University of California Press. 741−796

Gray H, 1977. Anatomy, Descriptive and Surgical. New York: Gramercy Books. 1−1257

Kaakinen A, Lunkka J P, 2003. Sedimentation of the Late Miocene Bahe Formation and its implications for stable environments adjacent to Qinling Mountain in Shaanxi, China. J Asian Earth Sci, 22: 67−78

Kaakinen A, Sonninen E, Lunkka J P, 2006. Stable isotope record in paleosol carbonates from the Chinese Loess Plateau: implications for late Neogene paleoclimate and paleovegetation. Palaeogeogr, Palaeoclimatol, Palaeoecol, 237: 359−369

Kurtén B, 1952. The Chinese *Hipparion* fauna – a quantitative survey with comments on the ecology of the machairodonts and hyaenids and the taxonomy of the gazelles. Soc Sci Fenn Comment Biol, 13: 1−82

Osborn H F, 1929. The titanotheres of ancient Wyoming, Dakota and Nebraska. US Geol Surv Monogr, 55: 1−953

Passey B H, Eronen J T, Fortelius M et al., 2007. Paleodiets and paleoenvironments of Late Miocene gazelles from North China: evidence from stable carbon isotopes. Vert PalAsiat, 45(2): 118−127

Pilgrim G E, 1937. Siwalik antelopes and oxen in the American Museum of Natural History. Bull Am Mus Nat Hist, 72: 729−847

Schlosser M, 1903. Die fossilen Säugethiere Chinas nebst einer Odontographie der recenten Antilopen. Abh Bayer Akad Wiss, 22: 1−221

Sisson S, 1914. The Anatomy of the Domestic Animals. Philadelphia: W.B. Saunders Company. 1−930

Teilhard de Chardin P, Trassaert M, 1938. Cavicornier of South-Eastern Shansi. Palaeont Sin, New Ser C, 6: 1−99

Teilhard de Chardin P, Young C C, 1931. Fossil mammals from northern China. Palaeont Sin, Ser C, 9(1): 1−66

Xia L, Yang Q S, Feng Z J et al., 2005. A guide to the measurement of mammal skull II: Perissodactyla, Artiodactyla and Carnivora. Chinese J Zool, 40(6): 67−73

Yang Q S, Xia L, Ma Y et al., 2005. A guide to the measurement of mammal skull I: basic measurement. Chinese J Zool, 40(3): 50−56

Zhang Z Q, 2003. A new species of *Shaanxispira* (Bovidae, Artiodactyla, Mammalia) from the Bahe Formation, Lantian, China. Vert PalAsiat, 41(3): 230−239

Zhang Z Q, 2006. Chinese late Neogene land mammal community and the environmental changes of east Asia. Vert PalAsiat, 44(2): 133−142

Zhang Z Q, Liu L P, 2005. The late Neogene mammal biochronology in the Loess Plateau, China. Ann Paléont, 91: 257−266

Zhang Z Q, Gentry A W, Kaakinen A et al., 2002. Land mammal faunal sequence of the Late Miocene of China: new evidence from Lantian, Shaanxi Province. Vert PalAsiat, 40(2): 165−177

Zhang Z Q, Kaakinen A, Liu L P et al., 2013. Mammalian biochronology of the Late Miocene Bahe Formation. In: Wang X M, Flynn L J, Fortelius M eds. Fossil Mammals of Asia − Neogene Biostratigraphy and Chronology. New York: Columbia University Press. 187−202